

Excellent electrochemical performance of nitrogen-enriched hierarchical porous carbon electrodes prepared using nano-CaCO₃ as template

Tingting Li · Guangwen Yang · Jing Wang ·
Yuanyuan Zhou · Heyou Han

Received: 7 May 2013 / Revised: 18 June 2013 / Accepted: 23 June 2013 / Published online: 6 July 2013
© Springer-Verlag Berlin Heidelberg 2013

Abstract Recently, tremendous research efforts have been concentrated on developing high-performance electrode materials to meet the ever-increasing energy and power demands in supercapacitors. Herein, we presented a high-capacity supercapacitor material based on nitrogen-enriched hierarchical porous carbons (NHPCs) synthesized by the carbonization of melamine formaldehyde resins using eco-friendly and inexpensive nano-CaCO₃ as template. The effects of carbonization temperature and template content on the porous structure and electrochemical characteristics were compared and discussed in detail. The prepared NHPCs possessed large surface area up to 834 m² g⁻¹ and high nitrogen content up to 20.94 wt %. As electrode material for supercapacitors, NHPCs exhibited superior electrochemical performances with high specific capacitance (190 F g⁻¹ at 20 A g⁻¹), outstanding rate capability (80 %), and excellent cycling stability (over 2,000 cycles at 5 A g⁻¹) in 1 M sulfuric acid media. The excellent electrochemical performances are due to the synergic effects of unique hierarchical porous microstructure, abundant nitrogen and oxygen functionalities, as well as high degree of graphitization framework.

Keywords Nitrogen doping · Hierarchical porous carbon · Nano-CaCO₃ · High capacitance · Supercapacitor

Introduction

As a new type of energy storage devices, supercapacitors have provoked tremendous attention because of their distinctive merits like long cycle life, high power capability, low

maintenance, and fast dynamics of charge propagation. Given these advantages, they promise to play a crucial role in meeting the demand of electronic devices both now and future [1–3]. It is known that the performance of supercapacitors depends intimately on the physical and chemical properties of their electrode materials, so more and more efforts have been contributed to explore desired electrode materials for supercapacitors [4, 5]. To date, porous carbon holds great promise as electrode material owing to their excellent conductivity, quite stable physicochemical properties, easy processability, controllable porosity, and low price [6–10]. Previous reports also showed using porous carbon as electrodes still suffered from several regrettable drawbacks, such as low power density and poor specific capacitance [4, 11]. The introduction of metal oxides and heteroatoms into carbon framework can compensate these defects due to their outstanding pseudo-capacitance effect. However, metal oxides are either too expensive (e.g., RuO₂) or poorly conductive (e.g., NiO) [12]. More recently, increasing research efforts have been focused on the modification of carbon materials with various heteroatoms, which can improve the surface wettability of the materials and generate high pseudo-capacitance while maintaining the superb cycle ability [13, 14]. Among them, nitrogen is superior because it has five valence electrons to attract protons and can enhance the charge density of the space-charge layer [13]. Especially, the N-enriched carbon acquired by employing N-enriched materials as precursors can realize a homogeneous incorporation and enjoy stable pseudo-capacitance properties.

On the other hand, hierarchically porous morphological characteristics with well-defined macropores and interconnected meso- and/or micropores are highly desirable for electrode materials, which provide fast ion and electron transfer and large reaction surface area, resulting in fast reaction kinetics [7, 10, 12, 15]. However, to date, the hierarchical structure is typically obtained by the impregnation of expensive macro-/mesoporous templates (e.g., porous solid silica [10, 16, 17] and zeolites [18,

T. Li · G. Yang · J. Wang · Y. Zhou · H. Han (✉)
State Key Laboratory of Agricultural Microbiology, College of
Science, Huazhong Agricultural University, 1 Shizishan Street,
Wuhan 430070, People's Republic of China
e-mail: hyhan@mail.hzau.edu.cn

19]) with the carbon precursor sols, followed by precursor carbonization and removal of templates, and/or then undergo activation processing to get a large number of micropores [19, 20]. Nevertheless, these templates have to be synthesized before use and be dissolved by strong acids (e.g., HF acid) after carbonization which is cumbersome and involve harsh experimental conditions. Activation treatment is time consuming because it usually requires secondary carbonization. Hence, an alternative template or a more affordable and simple method for preparing high surface area hierarchical porous carbon is highly desirable.

Inspired by these results, we prepared nitrogen-enriched hierarchical porous carbons (NHPCs) as electrode materials for supercapacitor by carbonization of melamine formaldehyde (MF) resins using nano- CaCO_3 as template. By varying preparation conditions (e.g., the carbonization temperature and template content), a series of samples with different N content or porous structure were obtained. The morphology and electrochemical properties of the carbon products were compared and discussed in detail. Combining the advantages of high-level N and O doping, unique hierarchical porous nanostructure, and localized graphitic structure, the NHPCs exhibited favorable electrochemical properties, making it suitable for high-performance supercapacitor application.

Experimental

Materials and synthesis

The NHPCs were prepared using the method previously reported by our group [21]. Briefly, to a stirred solution of formaldehyde (50 mL, Sinopharm Chemical Reagent Co., Ltd.), melamine was added (31.5 g, Tianjin Guangfu Fine Chemical Research Institute, 99.5 %) at room temperature. The pH of the mixture was adjusted to 8–9 by adding diluted NaOH (Tianjin Chemical Reagent Works), and then the mixture was stirred at 80 °C for 20 min to obtain a clear solution. After adjusting the solution to pH 5–6 by diluted HCl (Xinyang Chemical Works, 36 %), varying amounts (35–60 g) of hydrophilic nano- CaCO_3 (Shanxi Xintai NanoMater) were added under vigorous stirring. In order to obtain a homogeneous solution, a small amount of water was added appropriately, and continuous stirring was done until the solution solidified. Next, the resultant solids were left to dry at 60 °C in air and were then slowly heated to 180 °C overnight. The resultant dark brown composite was carbonized at desired temperature (800–1,000 °C) for 2 h under N_2 flow, with a heating rate of 5 °C min^{-1} . After cooling to room temperature, the resulting CaO/carbon composites were ground to fine powders and then stirred in diluted HCl for 24 h. The product was isolated by suction filtration, washed with deionized water, and then dried in a vacuum oven at 150 °C for 10 h. The resultant NHPC was denoted as NHPC- x - y , where x ($x=35, 50, 60$) and y

($y=800, 900, 1,000$) are the weight of CaCO_3 added and carbonization temperature, respectively.

Characterization

Scanning electron microscopy (SEM) images were taken by a JEOL JSM-6700F field emission scanning electron microscope. Transmission electron microscopy (TEM) images were performed on JEM-2010 with microscope operating at 200 kV. Elemental analyses were performed with an Elementar Vario Micro-cube elemental analyzer. N_2 adsorption–desorption isotherms were measured at 77 K on an Autosorb-1 from Quantachrome Instruments. The specific surface area was calculated from the adsorption data in the relative pressure interval from 0.05 to 0.20 using the Brunauer–Emmett–Teller (BET) method. The pore size distribution curve was obtained from desorption branch using Barrett–Joyner–Halenda (BJH) method. The total pore volume (V_{total}) was calculated at the relative pressure of 0.99. The micropore volume (V_{micro}) was determined from desorption branch at the relative pressure of 0.1. X-ray photoelectron spectra (XPS) were measured by a Thermo VG Multilab 2000 spectrometer equipped with a monochromatic Al K α radiation source at room temperature. Binding energies for the high-resolution spectra were calibrated by setting C 1s at 284.6 eV. X-ray diffraction (XRD) measurement was performed on a Rigaku D/MAX-rA diffractometer with Cu K α radiation ($\lambda=1.5406 \text{ \AA}$). Raman spectra were recorded by a Renishaw inVia Raman spectrometer equipped with a He–N laser excitation source operating at 632.8 nm.

Electrode preparation

The carbon material, polytetrafluoroethylene, and carbon black powder were mixed in a mass ratio of 8:1:1. The mixture was rolled into a thin film with a roller until the thickness was ca. 100 μm and was dried at 110 °C for 8 h. Then, the film was cut into a suitable shape and coated on 1 cm \times 1 cm platinum net which was used as the current collector. Finally, the ensemble was pressed together under about 10 MPa. The sample weight of each electrode was between 3 and 5 mg.

Electrochemical measurements

Cyclic voltammetry (CV), galvanostatic charge/discharge cycling (GC), and electrochemical impedance spectroscopy (EIS) were recorded using a CHI 660D electrochemical workstation. The GC result was employed in the evaluation of capacitance of each sample. All experiments were carried out at room temperature in a standard three electrode system, where platinum foil and Ag/AgCl were used as the counter and the reference electrode, respectively. Sulfuric acid (1 M) was used as the electrolyte. Before the test, the electrodes were

immersed in the electrolyte for 24 h. The specific gravimetric capacitance (C_g) was calculated from discharge process of the third cycle in a potential range of -0.1 to 1 V, calculated according to the following equation [22]: $C_g = I\Delta t / \Delta V$, where C_g is the specific gravimetric capacitance ($F\ g^{-1}$), I is the current density ($A\ g^{-1}$), Δt is the discharge time (s), and ΔV is the voltage window (1.1 V in this study).

Results and discussion

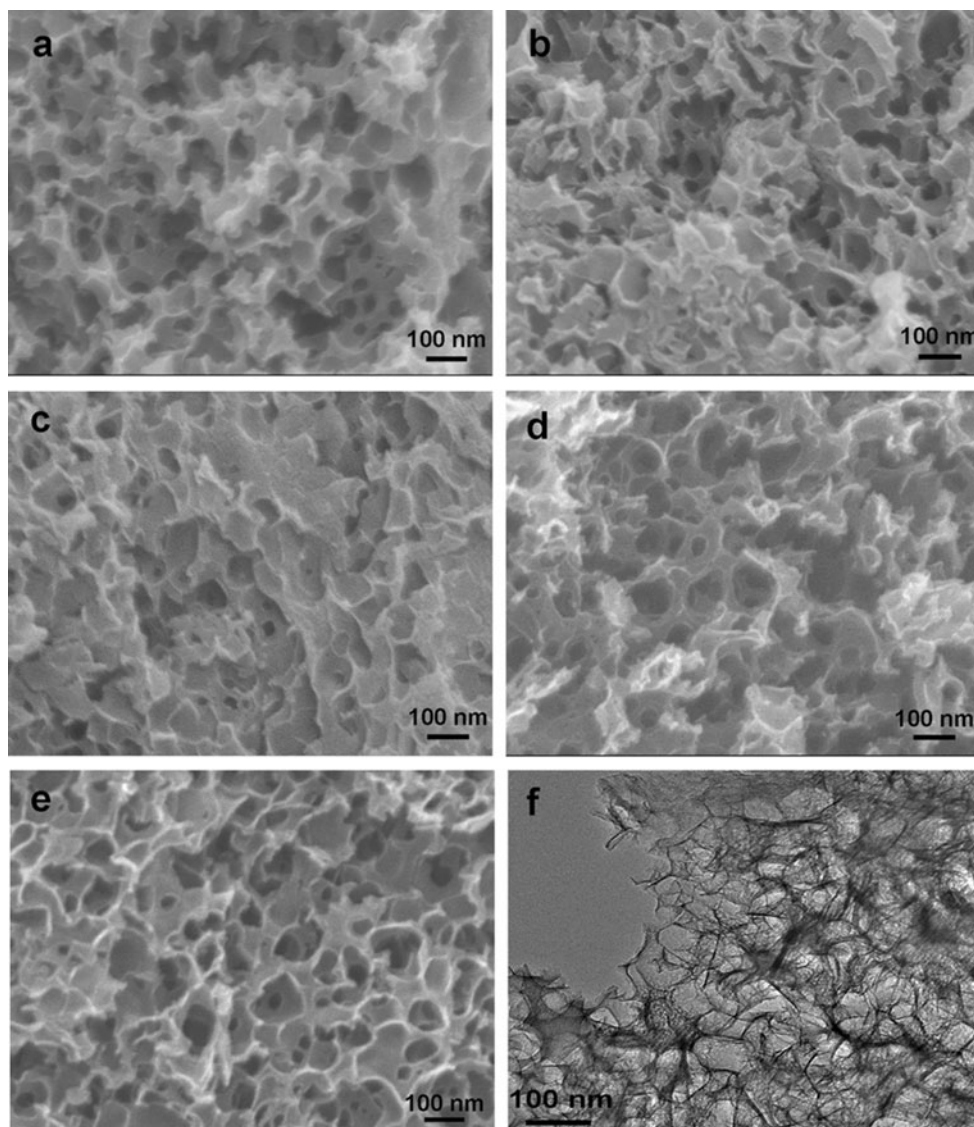
Morphology and structure characterization

The SEM and TEM images of the NHPCs are shown in Fig. 1. As reflected in Fig. 1a, NHPC-35-800 had more irregular pores, which were associated with high N content [23]. Particularly, in the SEM observation of NHPC-35-

1,000 (Fig. 1c), the morphology has undergone a slight change. The pore walls were thicker and legible layered structure appeared. Further investigation has been done to verify the influence of template content on porous structure. Compared with NHPC-35-900 (Fig. 1b), NHPC-50-900 (Fig. 1d) and NHPC-60-900 (Fig. 1e) presented more developed porous structure. Well-developed three-dimensional system of pores extended into the particles forming interconnected nanostructure, which is revealed by TEM image (Fig. 1f). Notably, this kind of pore structure was very important to improve the rate capability and large current charge/discharge performance, because they can facilitate better diffusion and transport of electrolyte [24].

To check the textural parameters of NHPCs, the materials were characterized by N_2 adsorption–desorption measurement (Fig. 2 and Table 1). As seen in Fig. 2a, the isotherms of all samples exhibited representative type II with H3 type

Fig. 1 SEM images of **a** NHPC-35-800, **b** NHPC-35-900, **c** NHPC-35-1,000, **d** NHPC-50-900, and **e** NHPC-60-900. **f** TEM image of NHPC-60-900



hysteresis loop and a sharp capillary condensation step at high relative pressures ($P/P_0=0.90-0.99$), implying the existence of large mesopores and macropores. It also can be confirmed in Fig. 2b, which displayed different intensity of peaks in the whole region (1–100 nm). The focused PSD peaks at the value of ~ 66 nm mainly derived from the strut of the CaO template. Micropores and small mesopores ascribed CO_2 activation and the intrinsic pores of carbon precursors. In addition, the sample carbonized at 900°C possessed larger specific surface area (see Table 1) because carbonization at 900°C can ensure the complete decomposition of CaCO_3 and samples are activated thoroughly. To explore the impact of template content on the structure and electrochemical performance, more CaCO_3 was introduced to the MF resin, followed by carbonization at 900°C . For NHPC- x -900 ($x=35, 50, 60$), V_{micro} increased greatly when the CaCO_3 amount in the CaCO_3 -MF composites is increased, indicating that the CO_2 activation can play a significant role in improving

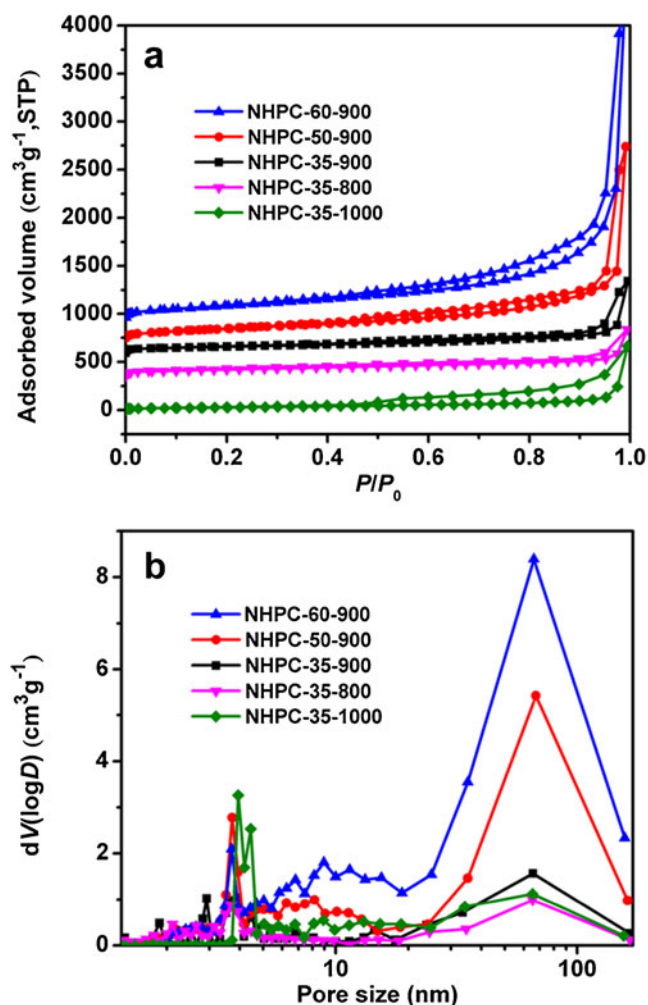


Fig. 2 a N_2 adsorption/desorption isotherms and b corresponding BJH PSDs of NHPC-35-800, NHPC-35-900, NHPC-35-1,000, NHPC-50-900, and NHPC-60-900

Table 1 BET specific area and porous texture of NHPCs materials

Sample	$S_{\text{BET}}/\text{m}^2\text{g}^{-1}$	$V_{\text{total}}/\text{cm}^3\text{g}^{-1}$	$V_{\text{micro}}/\text{cm}^3\text{g}^{-1}$	$V_{\text{micro}}^{\text{a}}/V_{\text{total}}^{\text{b}}$
NHPC-35-800	289	0.77	0.12	0.153
NHPC-35-900	321	1.17	0.09	0.080
NHPC-35-1,000	102	1.03	0.04	0.035
NHPC-50-900	658	3.23	0.25	0.077
NHPC-60-900	834	5.64	0.31	0.055

BET specific surface area

^a Micropore volume calculated from N_2 adsorption at $P/P_0 \approx 0.1$

^b Total pore volume calculated from N_2 adsorption at $P/P_0 \approx 0.99$

the microporous textures. Although V_{total} continued to increase, $V_{\text{micro}}/V_{\text{total}}$ gradually reduced. This is due to the fact that abundant CO_2 , serving as an activating gas, can connect pores, which makes part of micropore transform into mesopores.

Table 2 compiles the composition of all samples from elemental analysis. It can be seen that with increasing carbonization temperature, the content of C element increased, and in contrast, the N content was reduced. Here, we also examined whether the template ratio can affect the N content. For NHPC- x -900 ($x=35, 50, 60$), the relative content of various elements changed slightly, and the molar ratios of C/N were almost unchanged, so we can conclude that the weight ratio of nano- CaCO_3 to MF had little effect on the N content. In addition, elemental analysis results showed that enriched oxygen element is also present in the samples. Relatively speaking, the O content of all samples changed little and was derived from resin precursor and the introduction during chemical activation process. These accessible N and O species would provide the main active sites for pseudo-capacitive interaction.

It is necessary to clarify the transformation of N species introduced onto the porous carbon surface. N 1s spectra of NHPC-35- y were shown in Fig. 3 and fitted by four component peaks, which were assigned to pyridinic-like (N-6;

Table 2 Composition of NHPCs materials from elementary analysis

Sample	Chemical composition (%)			
	C	N	O	C/N
NHPC-35-800	62.3	20.9	15.0	3.48
NHPC-35-900	70.7	10.9	16.9	7.57
NHPC-35-1,000	80.6	6.4	12.5	14.69
NHPC-50-900	72.3	11.2	14.6	7.53
NHPC-60-900	73.9	11.3	13.4	7.63

C/N molar ratio

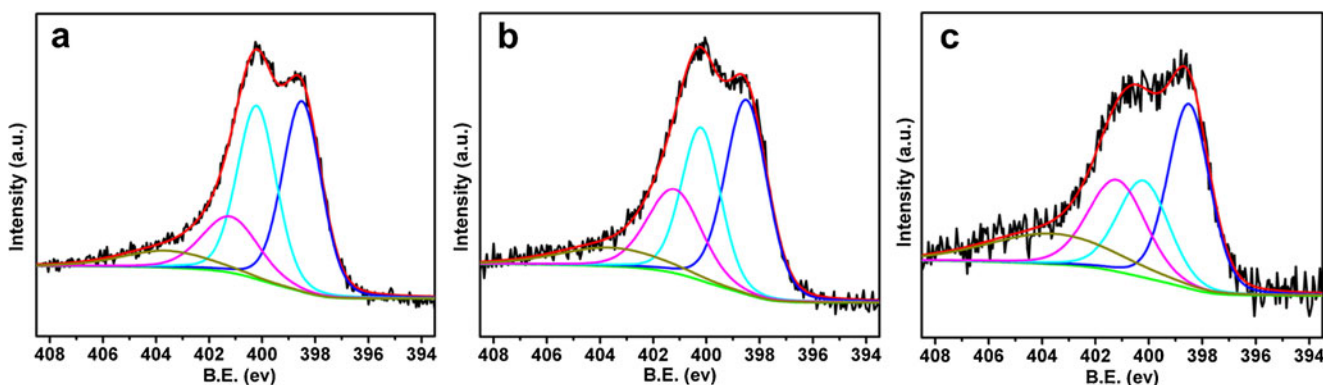


Fig. 3 XPS N 1s spectrum of **a** NHPC-35-800, **b** NHPC-35-900, and **c** NHPC-35-1,000, the meanings of different colored lines was raw intensity (black), fitting intensity (red), background (green), N-6 peak (blue), N-5 peak (cyan), N-Q peak (magenta) and N-O peak (dark yellow)

398.5±0.3 eV), pyrrolic-like (N-5; 400.2±0.3 eV), quaternary (N-Q; 401.2±0.3 eV), and oxidized (N-O; 403.6 eV) N species [25]. Interestingly, there is not much change in the intensity of N-6 peak for NHPC-35-800 (Fig. 3a), NHPC-35-900 (Fig. 3b), and NHPC-35-1,000 (Fig. 3c). However, further increase of carbonization temperature weakened the intensity of the N-5 peaks and obviously increased the intensities of N-O and N-Q peaks. These results indicated that a portion of N-5 had been chemically transformed into nitrogen species with higher binding energies during carbonization [26]. The percentages of N in NHPC-35- γ ($\gamma=800, 900, 1,000$) were calculated to be around 17.9, 9.4, and 4.6 %, respectively. It is worth noting that these values were lower than those from elemental analysis, intimating less N species on the external surface of the materials [27].

The samples were further analyzed by XRD in the wide-angle region (Fig. 4a). There are two diffraction peaks located at around 25° and 43°, which can be assigned, respectively, to the (002) and (101) planes of graphitic carbon [27, 28]. The narrowest and highest intensity peak suggested that NHPC-35-1,000 possessed the highest degree of graphitization [29]. This connection is further supported by Raman spectra (Fig. 4b). The ratios of the integrated D-band (~1,330 cm⁻¹) and G-band (~1,580 cm⁻¹) intensities were 1.14, 1.05, and 0.92

for NHPC-35-800, NHPC-35-900, and NHPC-35-1,000, respectively. A linear decrease in the intensity ratios of D to G band with temperature rising on one hand suggested that graphitization degree increased, on the other hand also explained the amount of disorder and number of defective sites decreased [30]. In addition to NHPC-35-1,000, low-intensity diffraction peaks of (004) around 53° were similarly observed in the XRD patterns of NHPC-50-900 and NHPC-60-900, which were caused by catalytic graphitization effect of the nano-CaCO₃. It also reflects the graphitization level and the characteristic of graphitic structures [21]. Moreover, peak intensity and template ratio present positive correlation. The graphite framework of NHPC-60-900 and NHPC-35-1,000 can be obviously discerned from Fig. 5a, b.

Electrochemical properties of NHPCs

NHPC electrodes were first characterized by CVs. Almost perfect rectangular-like CV curves in the whole voltage range (Fig. 6a, b) were mainly attributed to electronic double-layer effect [31]. The fast charge–discharge responses at the beginning of both positive and negative sweeps indicated that the NHPCs had suitable pore structures for easy ion transfer [32, 33]. Taking into account the fact that these perfect pores were obtained from duplication

Fig. 4 **a** XRD patterns of all samples and **b** Raman spectra of NHPC-35- γ showed the D and G band

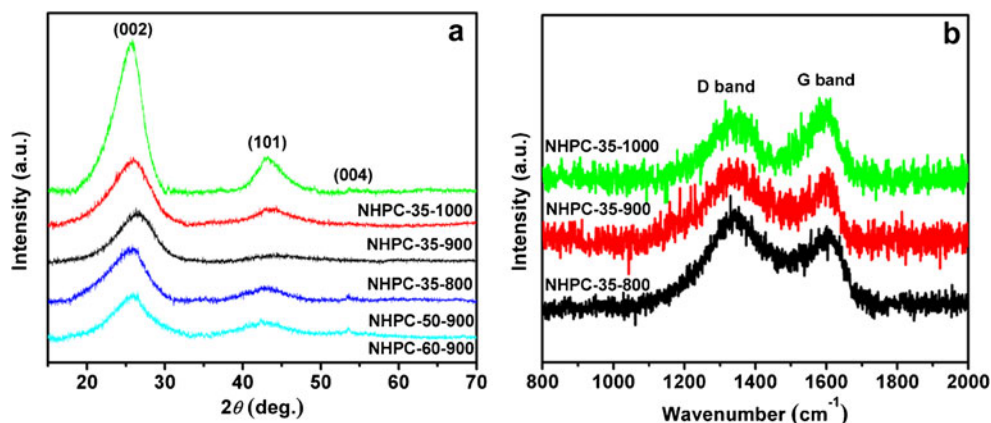
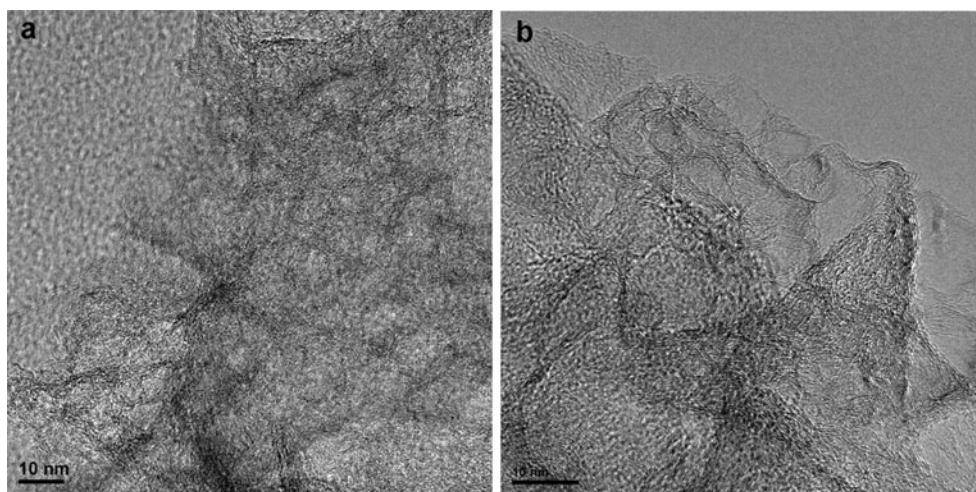
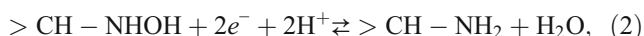


Fig. 5 HRTEM images of **a** NHPC-60-900 and **b** NHPC-35-1,000



process of the template, we believe that nano- CaCO_3 is a very potential template candidate for the preparation of porous carbon electrode. Besides, broad redox humps along the current–potential axis were observed, which were related to the surface functional groups (nitrogenated and oxygenated functionalities), implying that Faradaic reactions happened on the electrode surface [34, 35]. The offset of the peaks position and the width of these peaks suggested that various redox processes happened and overlapped. The redox reaction mechanism of nitrogen involved attracting protons and causing the transfer of charge. The charge transfer reactions are shown in the following equations [36]:



where $>\text{C}$ stands for the carbon network.

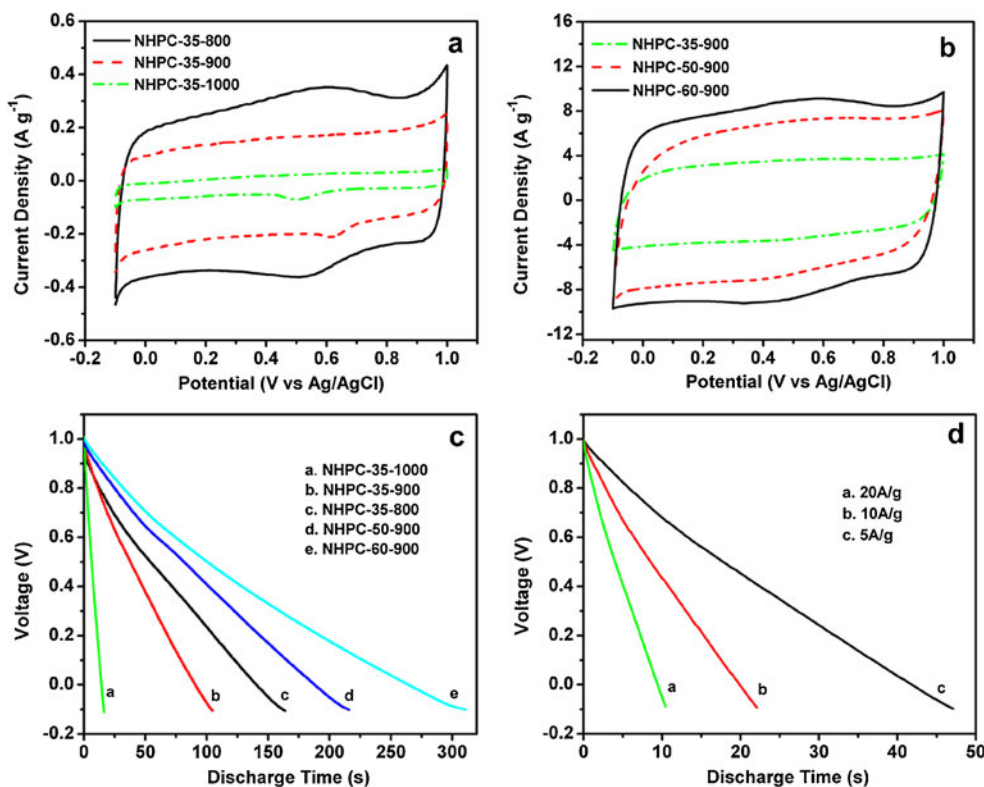
In Fig. 6a, NHPC-35-800 presented the largest curve area, symbolizing the highest capacitance value [16, 27]. The same circumstance happened to NHPC-60-900 (Fig. 6b). The superior capacitive behavior for the former was attributed to the predominant contribution of surface richer nitrogen and oxygen functionalities, the much higher capacitance of the latter derived from the perfect hierarchical porous structure with larger surface area.

The capacitance characteristics of obtained NHPCs were further investigated by GC experiments which were performed with the same voltage windows as the CV analysis above. Discharge curves of synthesized carbon materials at the same current density of 1 A g^{-1} are shown in Fig. 6c. In general, the $V-t$ relationships were approximately linear, indicating that the NHPCs electrodes behaved as a capacitor and gave high values of charge–discharge efficiency [16]. The specific capacitance values measured at a constant current density of 1 A g^{-1} were calculated to be 150, 95, 15, 196,

and 283 F g^{-1} for NHPC-35-800, NHPC-35-900, NHPC-35-1,000, NHPC-50-900, and NHPC-60-900, respectively. They are comparable with those of the mica-templated melamine-based porous carbon ($47.9\text{--}204.8 \text{ F g}^{-1}$) in 1 M sulfuric acid at a current density of 0.02 A g^{-1} [26]. Particularly, the specific capacitance of NHPC-60-900 is much higher than that of the melamine-based mesoporous carbon sphere (211 F g^{-1}) using silica as template in 5 M sulfuric acid at a current density of 1 A g^{-1} [37]. NHPC-35-800 had a higher capacitance value than NHPC-35-900 even if it had a smaller surface area and O content. This reflected that nitrogen-containing functional groups play crucial roles in capacitance enhancement. NHPC-60-900 displayed much outstanding capacitance due to facile ion migrations by the optimized hierarchical porous features. The hierarchical pores can exhibit a synergistic effect during the electrochemical charge–discharge process. The macropores served as ion-buffering reservoirs, minimizing the diffusion distances to the interior surfaces. The mesopores provided low-resistant pathways for ion transport, and the micropores enhanced the electrical double layer capacitance [12]. Therefore, the hierarchical porous structure with higher surface area may allow more N-containing and O-containing functional groups available for interaction with other species. In addition, further improvement of the carbonization temperature caused the significant decrease of the surface area and N-doped level. As a result, the capacitance value of NHPC-35-1,000 seriously decreased [38].

As revealed in Fig. 6d, under the current densities of 5, 10, and 20 A g^{-1} , NHPC-60-900 provided the corresponding specific capacitance values of 214, 201, and 190 F g^{-1} . The excellent capacitive values were markedly larger than those of previously reported hierarchical mesoporous carbon spheres (ca. $150\text{--}175 \text{ F g}^{-1}$ in 2.0 M sulfuric acid electrolyte) [10] and activated ordered mesoporous carbon (ca. $100\text{--}160 \text{ F g}^{-1}$ in 6.0 M KOH electrolyte) [20] electrodes at the same current

Fig. 6 CVs of **a** NHPC-35-800, NHPC-35-900, and NHPC-35-1,000 at a scan rate of 2 mV s^{-1} , **b** NHPC-35-900, NHPC-50-900, and NHPC-60-900 at a scan rate of 50 mV s^{-1} . Discharge curves of **c** NHPCs used as electrodes measured at a constant current density of 1 A g^{-1} , **d** NHPC-60-900 used as electrode measured at different current densities: 5, 10, and 20 A g^{-1} in the voltage range of $-0.1 \sim 1.0 \text{ V}$ vs. Ag/AgCl in 1 M sulfuric acid



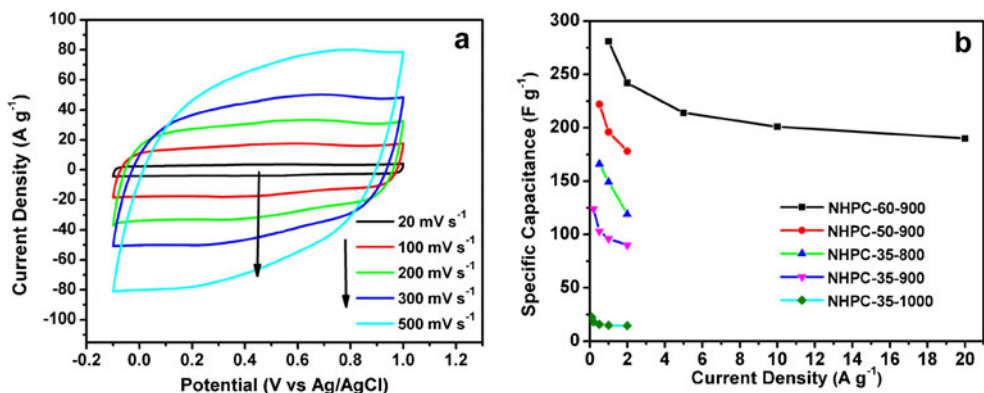
densities. No appreciable internal resistance drops were observed in the discharge curves even under higher current densities. It also can be observed that NHPC-60-900 still kept the “rectangular shape” CV even at higher scan rates (see Fig. 7a). These results highlighted the suitability of NHPC-60-900 for high-rate operation and low equivalent series resistance [4].

The dependence of the gravimetric capacitance on the current density is presented in Fig. 7b. A slight decrease of the specific capacitances was discovered for all samples with the increase of current densities, but it was maintained quite well for NHPC-60-900 under higher current densities. It also can be seen that NHPC-35-800 gave the most dramatic drop in capacitance and possessed the worst rate capability. The probable reasons may include the scarce pores which hindered the ion transport and the increased contribution of

pseudo-capacitance, the rate capability of which was inferior to the double layer capacitance due to electrochemical polarization [39]. As a comparison, approximately 80 % of capacity retention of NHPC-60-900 electrode was acquired as the current density increased from 2 to 20 A g^{-1} , which was slightly lower than that of p-SWCNT electrode (82 % from 4 to 40 A g^{-1}) [31] and much higher than the MnO_2 nanowire/CNT composite electrode (60 % from 77 to 770 mA g^{-1}) [11] in aqueous electrolyte. These results indicated that NHPC-60-900 exhibited excellent rate capability and without kinetic limitation for the capacitance [40].

Figure 8 presents the charge–discharge cycles of NHPC-60-900 at a constant current density of 5 A g^{-1} . Apparently, it exhibited an excellent cyclical stability within 2,000 cycles. The result illustrated that the pseudo-capacitance related to the

Fig. 7 **a** CVs of NHPC-60-900 at different scan rates and **b** specific capacitances of all samples at different current densities



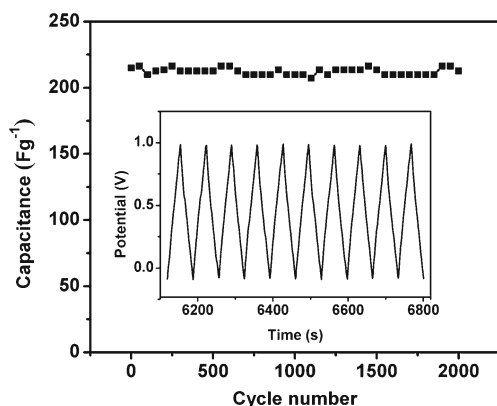


Fig. 8 Cycling stability and typical charge/discharge curves (inset) of the NHPC-60-900 at a current density of 5 A g^{-1} in 1 mol L^{-1} sulfuric acid electrolyte at room temperature

N-containing and O groups on the carbon surface and the electrical double layer capacitance derived from the hierarchical microstructure with high surface area were very stable.

The EIS of all samples are shown in Fig. 9a, b. The magnitude of the equivalent series resistance (ESR) obtained from the x intercept of the Nyquist plot was found to be as low as $0.65 \Omega \text{ cm}^{-2}$ for NHPC-35-1,000, whereas in the case of NHPC-35-800 and NHPC-35-900, the values were as high as 1.11 and $1.45 \Omega \text{ cm}^{-2}$, respectively (Fig. 9a). The improved electrical conductivity of NHPC-35-1,000 benefited from the higher degree of graphitization and/or the more ordered structure [12, 41]. Apart from this, the slopes of NHPC-35-800 and NHPC-35-900 in low frequency were smaller than that of NHPC-35-1,000 due to their greater Faradaic reaction [3]. The ESR for NHPC-60-900 was $0.61 \Omega \text{ cm}^{-2}$, which was smaller than those of NHPC-50-900 ($0.73 \Omega \text{ cm}^{-2}$) and NHPC-35-900 ($1.45 \Omega \text{ cm}^{-2}$) (Fig. 9b). A near-vertical linear shape of NHPC-60-900 in the low frequency region represented an ideal behavior and the lowest ion transfer resistance [33]. In previous reports, the ordered mesoporous carbon electrodes prepared by hard

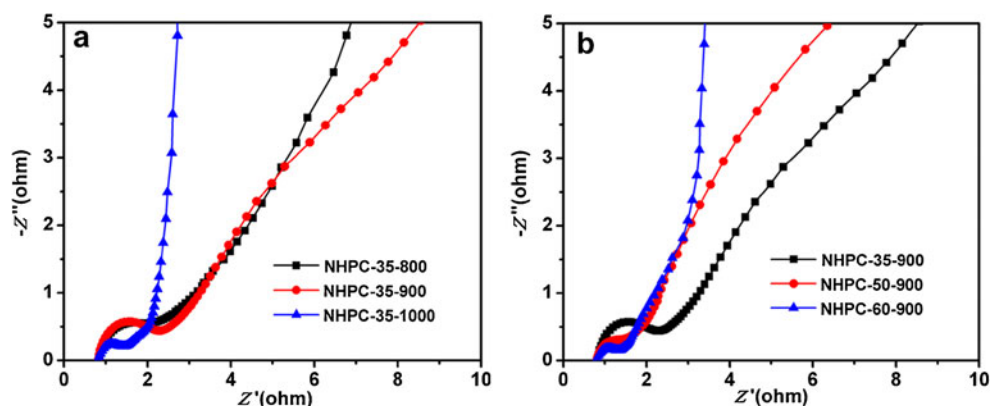
template method using CTAB/SiO₂, HMS, MCM-48, and SBA-15 displayed higher ESRs from 1.50 to $2.84 \Omega \text{ cm}^{-2}$ [42–44], which are larger than that of NHPCs (0.61 – $1.45 \Omega \text{ cm}^{-2}$) prepared here. The very low ESR was crucial for enhancing rate capability or the power density of the electrochemical capacitors [3].

As we all know, high degree of graphite structure plays an important role in providing porous carbon with excellent electronic conductivity [7]. Taking into account the above results and the catalytic graphitization effect of nano-CaCO₃ [21], the favorable electrochemical performances of NHPCs are likely attributed to the enriched N and O doping, unique hierarchical nanostructure, together with high degree of graphitization framework.

Conclusions

NHPCs were prepared with high N content, hierarchical porous structure, and excellent electrochemical performances. The effects of carbonization temperature and template content on the porous structure and electrochemical characteristics were compared and discussed in detail. As the electrode material for supercapacitors, NHPCs demonstrated superhigh electrochemical capacitance (190 F g^{-1} at the current density of 20 A g^{-1}), good rate capability (80 %), low impedance, and excellent cycling stability (2,000 cycles). The excellent electrochemical performances of NHPCs can be attributed to the combined effects of high N and O doping level (which augmented the double-layer capacitance with substantial redox pseudo-capacitance), hierarchical porous structure (which speeded up the rate of ion transfer and reduced the inner resistance of the electrodes), and high degree of graphitization framework (which provided porous carbon with excellent electronic conductivity). Our results showed that NHPCs would be promising choice for supercapacitors to meet the requirements of future energy and power storage devices.

Fig. 9 EIS of **a** NHPC-35- y and **b** NHPC- x -900 recorded in 1 M sulfuric acid, measured in the frequency range from 100 kHz to 10 mHz with an alternating current amplitude of 5 mV



Acknowledgments The authors gratefully acknowledge the support from the National Natural Science Foundation of China (grant numbers 20975042 and 21175051), the Fundamental Research Funds for the Central Universities (grant numbers 2010PY009 and 2011PY139), and the Natural Science Foundation of Hubei Province Innovation Team (grant number 2011CDA115).

References

- Miller JR, Simon P (2008) Materials science: electrochemical capacitors for energy management. *Science* 321:651–652
- Raymundo-Piñero E, Leroux F, Béguin F (2006) A high-performance carbon for supercapacitors obtained by carbonization of a seaweed biopolymer. *Adv Mater* 18:1877–1882
- Jeong HK, Jin M, Ra EJ, Sheem KY, Han GH, Arepalli S, Lee YH (2010) Enhanced electric double layer capacitance of graphite oxide intercalated by poly(sodium 4-styrenesulfonate) with high cycle stability. *ACS Nano* 4:1162–1166
- Chen LF, Zhang XD, Liang HW, Kong M, Guan QF, Chen P, Wu ZY, Yu SH (2012) Synthesis of nitrogen-doped porous carbon nanofibers as an efficient electrode material for supercapacitors. *ACS Nano* 6:7092–7102
- Davoglio RA, Biaggio SR, Bocchi N, Rocha-Filho RC (2013) Flexible and high surface area composites of carbon fiber, polypyrrole, and poly(DMcT) for supercapacitor electrodes. *Electrochim Acta* 93:93–100
- Frackowiak E, Béguin F (2001) Carbon materials for the electrochemical storage of energy in capacitors. *Carbon* 39:937–950
- Zhai Y, Dou Y, Zhao D, Fulvio PF, Mayes RT, Dai S (2011) Carbon materials for chemical capacitive energy storage. *Adv Mater* 23:4828–4850
- Wang DW, Li F, Chen ZG, Lu GQ, Cheng HM (2008) Synthesis and electrochemical property of boron-doped mesoporous carbon in supercapacitor. *Chem Mater* 20:7195–7200
- Stein A, Wang Z, Fierke MA (2009) Functionalization of porous carbon materials with designed pore architecture. *Adv Mater* 21:265–293
- Li Q, Jiang R, Dou Y, Wu Z, Huang T, Feng D, Yang J, Yu A, Zhao D (2011) Synthesis of mesoporous carbon spheres with a hierarchical pore structure for the electrochemical double-layer capacitor. *Carbon* 49:1248–1257
- Chou SL, Wang JZ, Chew SY, Liu HK, Dou SX (2008) Electrodeposition of MnO₂ nanowires on carbon nanotube paper as free-standing, flexible electrode for supercapacitors. *Electrochem Commun* 10:1724–1727
- Wang DW, Li F, Liu M, Lu GQ, Cheng HM (2008) 3D aperiodic hierarchical porous graphitic carbon material for high-rate electrochemical capacitive energy storage. *Angew Chem Int Ed* 47:373–376
- Wang DW, Li F, Yin LC, Lu X, Chen ZG, Gentle IR, Lu GQ, Cheng HM (2012) Nitrogen-doped carbon monolith for alkaline supercapacitors and understanding nitrogen-induced redox transitions. *Chem Eur J* 18:5345–5351
- Hulicova-Jurcakova D, Kodama M, Shiraishi S, Hatori H, Zhu ZH, Lu GQ (2009) Nitrogen-enriched nonporous carbon electrodes with extraordinary supercapacitance. *Adv Funct Mater* 19:1800–1809
- Gutiérrez-Sánchez C, Jia W, Beyl Y, Pita M, Schuhmann W, De Lacey AL, Stoica L (2012) Enhanced direct electron transfer between laccase and hierarchical carbon microfibers/carbon nanotubes composite electrodes. Comparison of three enzyme immobilization methods. *Electrochim Acta* 82:218–223
- Yang X, Wu D, Chen X, Fu R (2010) Nitrogen-enriched nanocarbons with a 3-D continuous mesopore structure from polyacrylonitrile for supercapacitor application. *J Phys Chem C* 114:8581–8586
- Xu J, Luan Z, He H, Zhou W, Kevan L (1998) A reliable synthesis of cubic mesoporous MCM-48 molecular sieve. *Chem Mater* 10:3690–3698
- Ania CO, Khomenko V, Raymundo-Piñero E, Parra JB, Béguin F (2007) The large electrochemical capacitance of microporous doped carbon obtained by using a zeolite template. *Adv Funct Mater* 17:1828–1836
- Wang H, Gao Q, Hu J (2010) Preparation of porous doped carbons and the high performance in electrochemical capacitors. *Microporous Mesoporous Mater* 131:89–96
- Lv Y, Zhang F, Dou Y, Zhai Y, Wang J, Liu H, Xia Y, Tu B, Zhao D (2012) A comprehensive study on KOH activation of ordered mesoporous carbons and their supercapacitor application. *J Mater Chem* 22:93–99
- Yang G, Han H, Li T, Du C (2012) Synthesis of nitrogen-doped porous graphitic carbons using nano-CaCO₃ as template, graphitization catalyst, and activating agent. *Carbon* 50:3753–3765
- Jain A, Tripathi SK, Gupta A, Kumari M (2012) Fabrication and characterization of electrochemical double layer capacitors using ionic liquid-based gel polymer electrolyte with chemically treated activated charcoal electrodes. *J Solid State Electrochem* 17:713–726
- Chen Z, Higgins D, Tao H, Hsu RS, Chen Z (2009) Highly active nitrogen-doped carbon nanotubes for oxygen reduction reaction in fuel cell applications. *J Phys Chem C* 113:21008–21013
- Xu F, Cai R, Zeng Q, Zou C, Wu D, Li F, Lu X, Liang Y, Fu R (2011) Fast ion transport and high capacitance of polystyrene-based hierarchical porous carbon electrode material for supercapacitors. *J Mater Chem* 21:1970–1976
- Pels JR, Kapteijn F, Moulijn JA, Zhu Q, Thomas KM (1995) Evolution of nitrogen functionalities in carbonaceous materials during pyrolysis. *Carbon* 33:1641–1653
- Hulicova D, Yamashita J, Soneda Y, Hatori H, Kodama M (2005) Supercapacitors prepared from melamine-based carbon. *Chem Mater* 17:1241–1247
- Su F, Poh CK, Chen JS, Xu G, Wang D, Li Q, Lin J, Lou XW (2011) Nitrogen-containing microporous carbon nanospheres with improved capacitive properties. *Energy Environ Sci* 4:717–724
- Liu R, Wu D, Feng X, Müllen K (2010) Nitrogen-doped ordered mesoporous graphitic arrays with high electrocatalytic activity for oxygen reduction. *Angew Chem Int Ed* 49:2565–2569
- Paraknowitsch JP, Zhang J, Su D, Thomas A, Antonietti M (2010) Ionic liquids as precursors for nitrogen-doped graphitic carbon. *Adv Mater* 22:87–92
- Terrones M, Redlich P, Grobert N, Trasobares S, Hsu WK, Terrones H, Zhu YQ, Hare JP, Reeves CL, Cheatham AK, Rühle M, Kroto HW, Walton DRM (1999) Carbon nitride nanocomposites: formation of aligned C_xN_y nanofibers. *Adv Mater* 11:655–658
- Shen J, Liu A, Tu Y, Foo G, Yeo C, Chan-Park MB, Jiang R, Chen Y (2011) How carboxylic groups improve the performance of single-walled carbon nanotube electrochemical capacitors? *Energy Environ Sci* 4:4220–4229
- Xing W, Qiao SZ, Ding RG, Li F, Lu GQ, Yan ZF, Cheng HM (2006) Superior electric double layer capacitors using ordered mesoporous carbons. *Carbon* 44:216–224
- Liang Y, Wu D, Fu R (2009) Preparation and electrochemical performance of novel ordered mesoporous carbon with an interconnected channel structure. *Langmuir* 25:7783–7785
- Hu B, Qin X, Asiri AM, Alamry KA, Al-Youbi AO, Sun X (2013) WS₂ nanoparticles-encapsulated amorphous carbon tubes: a novel electrode material for supercapacitors with a high rate capability. *Electrochem Commun* 28:75–78
- Jagadale AD, Jamadade VS, Pusawale SN, Lokhande CD (2012) Effect of scan rate on the morphology of potentiodynamically deposited β-Co(OH)₂ and corresponding supercapacitive performance. *Electrochim Acta* 78:92–97
- Béguin F, Szostak K, Lotz G, Frackowiak E (2005) A self-supporting electrode for supercapacitors prepared by one-step pyrolysis of carbon nanotube/polyacrylonitrile blends. *Adv Mater* 17:2380–2384

37. Li W, Chen D, Li Z, Shi Y, Wan Y, Huang J, Yang J, Zhao D, Jiang Z (2007) Nitrogen enriched mesoporous carbon spheres obtained by a facile method and its application for electrochemical capacitor. *Electrochem Commun* 9:569–573
38. Bastakoti BP, Huang HS, Chen LC, Wu KCW, Yamauchi Y (2012) Block copolymer assisted synthesis of porous α -Ni(OH)₂ microflowers with high surface areas as electrochemical pseudocapacitor materials. *Chem Commun* 48:9150–9152
39. Xu B, Hou S, Cao G, Wu F, Yang Y (2012) Sustainable nitrogen-doped porous carbon with high surface areas prepared from gelatin for supercapacitors. *J Mater Chem* 22:19088–19093
40. Peng Y, Chen Z, Wen J, Xiao Q, Weng D, He S, Geng H, Lu Y (2010) Hierarchical manganese oxide/carbon nanocomposites for supercapacitor electrodes. *Nano Res* 4:216–225
41. Hulicova D, Kodama M, Hatori H (2006) Electrochemical performance of nitrogen-enriched carbons in aqueous and non-aqueous supercapacitors. *Chem Mater* 18:2318–2326
42. Yoon S, Jang JH, Ka BH, Oh SM (2005) Complex capacitance analysis on rate capability of electric-double layer capacitor (EDLC) electrodes of different thickness. *Electrochim Acta* 50:2255–2262
43. Lee J, Kim J, Lee Y, Yoon S, Oh SM, Hyeon T (2004) Simple synthesis of uniform mesoporous carbons with diverse structures from mesostructured polymer silica nanocomposites. *Chem Mater* 16:3323–3330
44. Yoon S, Oh SM, Lee CW, Ryu JH (2011) Pore structure tuning of mesoporous carbon prepared by direct templating method for application to high rate supercapacitor electrodes. *J Electroanal Chem* 650:187–195